Characterization of squeezed states with controllable coherent light injection at sidebands

Li Wei, Jin YuanBin and Yu XuDong

Citation: SCIENCE CHINA Physics, Mechanics & Astronomy **60**, 050321 (2017); doi: 10.1007/s11433-017-9021-7

View online: http://engine.scichina.com/doi/10.1007/s11433-017-9021-7

View Table of Contents:http://engine.scichina.com/publisher/scp/journal/SCPMA/60/5

Published by the Science China Press

SCIENCE CHINA
Physics, Mechanics & Astronomy

SCIENCE CHINA
Physics, Mechanics & Astronomy

• Letter to the Editor •

May 2017 Vol. 60 No. 5: 050321
doi: 10.1007/s11433-017-9021-7

Characterization of squeezed states with controllable coherent light injection at sidebands

Wei Li[1,2], YuanBin Jin[1,2], and XuDong Yu[1,2*]

[1] *State Key Laboratory of Quantum Optics and Quantum Optics Devices, Institute of Opto-Electronics, Shanxi University, Taiyuan 030006, China;*
[2] *Collaborative Innovation Center of Extreme Optics, Shanxi University, Taiyuan 030006, China*

Received February 6, 2017; accepted March 14, 2017; published online March 23, 2017

Citation: W. Li, Y. B. Jin, and X. D. Yu, Characterization of squeezed states with controllable coherent light injection at sidebands, Sci. China-Phys. Mech. Astron. **60**, 050321 (2017), doi: 10.1007/s11433-017-9021-7

The squeezed state was experimentally produced in the four wave mixing process for the first time thirty years ago [1]. Its intrinsic nonclassical property has always attracted the attention of the scientists, and it has also presented an unpredictable application potential in quantum information processing [2-6] and quantum metrology [7-9]. For gaining an insight into the quantum state, Bertrand et al. [10] introduced the concept of quantum tomography into quantum mechanics in 1987. And in 1997, Breitenbach et al. [11] presented the noise distribution of the squeezed states of light fields and reconstructed the quantum states by balanced homodyne detection (BHD). If the squeezed state light field has a relatively strong amplitude, BHD is not suitable. Consequently, other approaches have also been studied, such as self-tomography of the twin-beam state [12] and self-tomography of the single-mode squeezed light field with an empty cavity [13]. These approaches enable people to understand the nature of the quantum state.

In this paper, we propose an alternative method to study the property of the squeezed state of the light field by making use of controllable coherent sideband injection [14-16] and provide experimental demonstration. In optical quantum tomography, for instance in ref. [11], an optical parametric oscillator (OPO) is usually fed by the fundamental frequency light field $\hat{a}^{\rm in}(\omega_0)$ with two symmetric sidebands $\hat{a}^{\rm in}_{\pm}(\omega_0 \pm \Omega)$ generated by electro-optic modulation. In our scheme, the two input sideband fields of the OPO generated by a frequency shift system as discussed in our previous papers [15, 17] have the same power, but their frequencies can be dissymmetric (one is located at $\Omega_1 = -5$ MHz around the fundamental light field (ω_0) and the other at $\Omega_2 = 5.0001$ or 5 MHz) and they are selectable by blocking or opening one of them or both. The output fields of the OPO are combined with a strong local oscillator at the fundamental frequency on a 50/50 beam splitter (BS) and the mixed modes of the BS are detected by two balanced detectors. The photocurrent subtraction of the detectors is mixed with a 5 MHz cosine wave from a function generator and the mixing signal after a low-pass filter is measured by an oscilloscope. The relative phase of the local beam and the detected field is controlled by a mirror mounted on a piezoelectric transducer (PZT). Thus, we can obtain the noise distribution of the quadrature component at an analysis frequency of 5 MHz. Contrasted to the traditional optical homodyne tomography, in our scheme, the single-sideband injection can present the noise distribution of the quantum state. Simultaneously, because of the beat signal caused by the different sideband frequencies and the different frequency demodulation, the properties of the coherent state and the squeezed states are more clearly presented.

The OPO is currently the most successful device used for generating the squeezed light field [18-20], and is generally composed of a resonator and a second-order ($\chi^{(2)}$) nonlinear crystal. In the ideal case (here we just consider the broad band squeezing because the sideband frequency is consider-

*Corresponding author (email: jiance_yu@sxu.edu.cn)

ably smaller than the linewidth of the OPO), the squeezing operator is written as $\hat{S}(r,\theta) = \exp[r(\hat{a}_+^{\rm in}\hat{a}_-^{\rm in}e^{-2i\theta} - \hat{a}_+^{\rm in\dagger}\hat{a}_-^{\rm in\dagger}e^{2i\theta})]$ (θ is the squeezing angle). In the phase space, the quadrature component vector of the output fields can be written as [21]:

$$\begin{pmatrix}\hat{X}^{\rm out}\\ \hat{Y}^{\rm out}\end{pmatrix} = \begin{pmatrix}A & B\\ B & C\end{pmatrix}\begin{pmatrix}\hat{X}^{\rm in}\\ \hat{Y}^{\rm in}\end{pmatrix}, \tag{1}$$

where $A = \cosh(r) + \sinh(r)\cos(2\theta)$, $B = \sinh(r)\sin(2\theta)$ and $C = \cosh(r) - \sinh(r)\cos(2\theta)$. $\hat{X}^{\rm in}$ and $\hat{Y}^{\rm in}$ are the quadrature amplitude and the quadrature phase of the input field, respectively. Consequently, when $\theta = 0$, the parametric interaction amplifies the quadrature amplitude and deamplifies the quadrature phase of the output field ($\hat{X}^{\rm out} = e^r\hat{X}^{\rm in}$, $\hat{Y}^{\rm out} = e^{-r}\hat{Y}^{\rm in}$). If $\theta = \pi/2$, the outgoing quadrature amplitude of the OPO is deamplified and the quadrature phase is amplified ($\hat{X}^{\rm out} = e^{-r}\hat{X}^{\rm in}$, $\hat{Y}^{\rm out} = e^r\hat{Y}^{\rm in}$).

Now, we consider the measurement scheme. The output field of the OPO is combined with a strong local oscillator (LO) at the fundamental frequency on a 50/50 BS and two balanced detectors measure the two mixed modes output from BS. The photocurrent subtraction of the balanced detectors can be written as:

$$\delta\hat{i}_- = \hat{a}_{\rm LO}^\dagger\hat{a}e^{-i\phi} + \hat{a}_{\rm LO}\hat{a}^\dagger e^{i\phi}, \tag{2}$$

where the LO field is seen as a classical field and can be expressed as $a_{\rm LO} = \alpha_{\rm LO}e^{-i\omega_0 t}$ ($\alpha_{\rm LO}$ is the classical amplitude and we assume that $\alpha_{\rm LO}$ is a real number).

Case 1. Suppose a single-sideband field $\hat{a}_{s1}^{\rm in}$ located at $\omega_1 = \omega_0 - \Omega_0$ (the mean amplitude of the input field $\alpha_{s1}^{\rm in}$ is a real number) is injected into the OPO, and the other input sideband field $\hat{a}_{i1}^{\rm in}$ at $\omega_0 + \Omega_0$ is the vacuum field ($\alpha_{i1}^{\rm in} = 0$). Hence, the mean value of the quadrature components of the input fields at the analysis frequency of Ω_0 $\langle\hat{X}^{\rm in}(\Omega_0)\rangle = \frac{\alpha_{s1}^{\rm in}}{\sqrt{2}}$ and $\langle\hat{Y}^{\rm in}(\Omega_0)\rangle = -\frac{\alpha_{s1}^{\rm in}}{i\sqrt{2}}$, and the fluctuation of the input quadrature component $\delta\hat{X}^{\rm in}(\Omega_0) = \frac{1}{\sqrt{2}}[\delta\hat{a}_{i1}^{\rm in}(\Omega_0) + \delta\hat{a}_{s1}^{\rm in\dagger}(-\Omega_0)]$ and $\delta\hat{Y}^{\rm in}(\Omega_0) = \frac{1}{i\sqrt{2}}[\delta\hat{a}_{i1}^{\rm in}(\Omega_0) - \delta\hat{a}_{s1}^{\rm in\dagger}(-\Omega_0)]$. The output field of the OPO is written as $\hat{a} = \hat{a}_{s1}^{\rm out}e^{-i(\omega_0-\Omega_0)t} + \hat{a}_{i1}^{\rm out}e^{-i(\omega_0+\Omega_0)t}$. Therefore, the photocurrent subtraction analyzed is

$$\begin{aligned}\delta\hat{i}_{-1}(\Omega_0) =& \alpha_{\rm LO}(\alpha_{s1}^{\rm out} + \alpha_{i1}^{\rm out})\cos[\phi(t)]\\ &+ \alpha_{\rm LO}[\delta\hat{X}_{s1}^{\rm out}(-\Omega_0) + \delta\hat{X}_{i1}^{\rm out}(\Omega_0)]\cos[\phi(t)]\\ &+ \alpha_{\rm LO}[\delta Y_{s1}^{\rm out}(-\Omega_0) + \delta Y_{i1}^{\rm out}(\Omega_0)]\sin[\phi(t)]\\ =& \alpha_{\rm LO}\{\alpha_{s1}^{\rm in}e^{\pm r}\cos[\phi(t)]\\ &+ \delta\hat{X}^{\rm in}(\Omega_0)e^{\pm r}\cos[\phi(t)]\\ &+ \delta Y^{\rm in}(\Omega_0)e^{\mp r}\sin[\phi(t)]\}.\end{aligned} \tag{3}$$

Case 2. The injected single sideband field with the real-value mean amplitude $\alpha_{s2}^{\rm in}$ is at $\omega_2 = \omega_0 + \Omega_0 + \Delta\Omega$. Therefore, the input mean values of the quadrature components at are $\Omega_0 + \Delta\Omega$ are $\langle\hat{X}^{\rm in}(\Omega_0 + \Delta\Omega)\rangle = \frac{\alpha_{s2}^{\rm in}}{\sqrt{2}}$ and $\langle\hat{Y}^{\rm in}(\Omega_0 + \Delta\Omega)\rangle = \frac{\alpha_{s2}^{\rm in}}{i\sqrt{2}}$ and the fluctuation at the arbitrary analysis frequency Ω are $\delta\hat{X}^{\rm in}(\Omega) = \frac{1}{\sqrt{2}}[\delta\hat{a}_{s2}^{\rm in}(\Omega) + \delta\hat{a}_{i2}^{\rm in\dagger}(-\Omega)]$ and $\delta\hat{Y}^{\rm in}(\Omega) = \frac{1}{i\sqrt{2}}[\delta\hat{a}_{s2}^{\rm in}(\Omega) - \delta\hat{a}_{i2}^{\rm in\dagger}(-\Omega)]$. Consequently the photocurrent subtraction at the analysis frequency of Ω_0 is

$$\begin{aligned}\delta i_{-2}(\Omega_0) =& \alpha_{\rm LO}\{\alpha_{s2}^{\rm out}\cos[\phi(t) - \Delta\Omega t]\\ &+ \alpha_{i2}^{\rm out}\cos[\phi(t) + \Delta\Omega t]\}\\ &+ \alpha_{\rm LO}[\delta X_{s2}^{\rm out}(\Omega_0) + \delta X_{i2}^{\rm out}(-\Omega_0)]\cos[\phi(t)]\\ &+ \alpha_{\rm LO}[\delta Y_{s2}^{\rm out}(\Omega_0) + \delta Y_{i2}^{\rm out}(-\Omega_0)]\sin[\phi(t)]\\ =& \alpha_{\rm LO}\{\pm\frac{1}{2}\left(e^r - \frac{1}{e^r}\right)\alpha_{s2}^{\rm in}\cos[\Delta\Omega t + \phi(t)]\\ &+ \frac{1}{2}\left(e^r + \frac{1}{e^r}\right)\alpha_{s2}^{\rm in}\cos[\Delta\Omega t - \phi(t)]\\ &+ \delta\hat{X}^{\rm in}(\Omega_0)e^{\pm r}\cos[\phi(t)]\\ &+ \delta Y^{\rm in}(\Omega_0)e^{\mp r}\sin[\phi(t)]\}.\end{aligned} \tag{4}$$

Case 3. Two dissymmetric sidebands located at $\omega_1 = \omega_0 - \Omega_0$ and $\omega_2 = \omega_0 + \Omega_0 + \Delta\Omega$, respectively, but with the same power, are injected into the OPO simultaneously. Hence, the output fields of the OPO contain two pairs of symmetrical sidebands whose frequencies are $\omega_0 \pm \Omega_0$ and $\omega_0 \pm \Omega_0 \pm \Delta\Omega$. Therefore, the photocurrent subtraction analyzed at the sideband frequency of Ω_0 can be expressed as:

$$\delta i_{-3}(\Omega_0) = \delta i_{-1}(\Omega_0) + \delta i_{-2}(\Omega_0). \tag{5}$$

In this case, $\Delta\Omega = 0$, corresponds to the injection of symmetric double sidebands, and is same as the traditional optical tomography scheme.

The experimental setup and the schematic diagram are shown in Figure 1(a) and (b). The diode-pumped intracavity frequency-doubled laser provides a fundamental light of 200 mW at 1064 nm and a second-harmonic light of 450 mW at 532 nm simultaneously. The infrared output at 1064 nm is split into two beams, one of which is served as local oscillator of the detection system after the mode-cleaning cavity (MC). The other beam is injected into the double-sidebands generation system that consists of three acoustic optical modulators (AOMs). AOM1 shifts the laser frequency by a amount of –110 MHz. The half-wave plate (HW2) and the polarization beam splitter (PBS2) split the frequency-shifted laser beam into two parts. The frequencies of the two parts are pulled in the conversion direction by AOM2 and AOM3 by the amounts of 105 and 115.0001 MHz (or 115 MHz) respectively. The two frequency-shifted beams are combined on BS1 and one of the two output fields of the BS is coupled into a single-mode polarization-maintaining optical fiber. To stabilize the frequency and phase of double sidebands, the clocks of the signal sources of the AOM drivers are synchronized [15, 17].

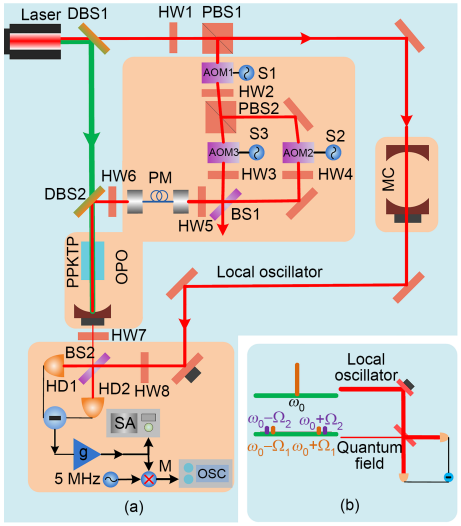

Figure 1 (Color online) (a) The experimental setup. AOM1-3: acoustic optical modulator; PM: single-mode polarization-maintaining optical fiber; HW1-8: half-wave plate; DBS1-2: dichroic beam splitter; PBS1-2: polarization beam splitter; BS1-2: 50/50 beam splitter; PPKTP: periodically poled potassium titanyl phosphate; OPO: optical parametric oscillator; M: mixer; SA: spectrum analyzer; OSC: oscilloscope; (b) schematic diagram of the detection scheme.

The output beam of the fiber is injected into the OPO, which is resonant for both the fundamental light and the second-harmonic light. The oscillator contains a type-I periodically poled potassium titanyl phosphate (PPKTP) crystal (1 mm×2 mm×10 mm) and the bandwidth of the OPO is approximately 70 MHz. The output field of the OPO is combined with the local oscillator on BS2. Two balanced detectors are utilized to measure the output lights of the BS. The amplified subtraction signal of the detectors is divided into two parts. One part is input to the spectrum analyzer (SA). The other is mixed with a 5 MHz radio frequency (RF) signal generated by a function generator and the demodulated signal after a low-pass filter is collected by the oscilloscope (OSC).

The noise traces of the quantum states at the demodulation frequency $\Omega_0 = 5$ MHz are listed in Figures 2 and 3. The power of the pump light is 30 mW and the classical gain of the parametric process is about 4 in our experiment when the fundamental frequency field at ω_0 is injected. The power of each injected sideband field is fixed as 10 nW in the three cases. Each trace has 1.2 million points as the relative phase $\phi(t)$ is swept by a mount of 4π in approximately 500 ms. In Figure 2(b)-(d) show the noise traces when the single sideband at –5 MHz is fed in the OPO, corresponding to case 1. Figure 2(b) is the coherent state as the pump field of the OPO is blocked. The coherent amplitude is proportional to $\alpha_s^{\rm in}$ and the noise amplitude corresponds to the vacuum fluctuation. Figure 2(c) is the result of the amplitude-squeezed state. In this case, the relative phase θ of the pump and the input signal field is $\pi/2$ and the OPO works in the anti-amplification condition. The phase difference of the output signal field and

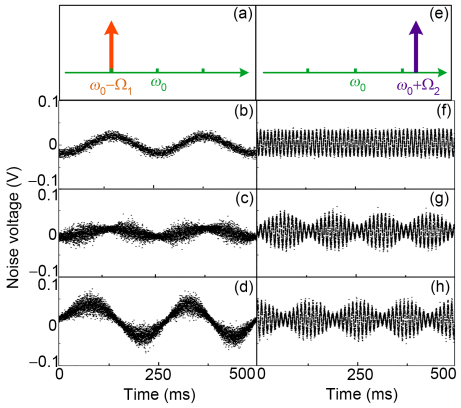

Figure 2 (Color online) The noise traces of the quantum states at the analysis frequency $\Omega_0 = 5$ MHz when the single sideband field is injected into the OPO. (a) and (e) are injected sideband fields described in sideband picture; (b)-(d) are the results of the coherent state, amplitude-squeezed state and phase-squeezed state when the sideband field $\hat{a}_{s1}^{\rm in}(\omega_0 - \Omega_0)$ is used; (f)-(h) show the results of the upper sideband field injection ($\hat{a}_{s2}^{\rm in}(\omega_0 + \Omega_0 + \Delta\Omega)$).

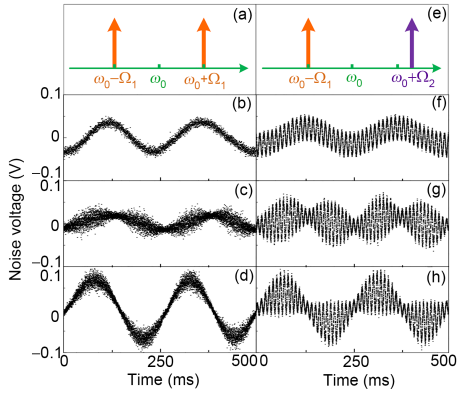

Figure 3 (Color online) The noise traces of the states at the analysis frequency $\Omega_0 = 5$ MHz when double sidebands are injected into the OPO. (a) and (e) are injected sideband fields described in sideband picture; (b)-(d) show the results for the coherent state, amplitude-squeezed state and phase-squeezed state when the frequency shift of AOM2 and AOM3 are 105 and 115 MHz; (f)-(h) show the corresponding results when the frequency shift of AOM2 and AOM3 are 105 and 115.0001 MHz respectively.

the idle field of the OPO is approximately equal to π and the fields are out of phase. Therefore, the mean amplitude of the squeezed light field is proportional to $|\alpha_{s1}^{\rm out}| - |\alpha_{i1}^{\rm out}| = {\rm e}^{-r}\alpha_{s1}^{\rm in} < \alpha_{s1}^{\rm in}$. Hence, the coherent amplitude of the amplitude-squeezed state is smaller than that in Figure 2(b). As shown in the figure simultaneously, the noise amplitude is smaller than that of the vacuum state when $\phi(t) = \pm n\pi$ ($n = 0, 1, 2, ...$) because the correlated noise amplitude $|\delta X_{s1}^{\rm out}(-\Omega_0) + \delta X_{i1}^{\rm out}(\Omega_0)| \simeq {\rm e}^{-r} < 1$. And the noise amplitude is larger than that of the vacuum state if $\phi(t) = \pm n\pi + \pi/2$, i.e., $|\delta Y_{s1}^{\rm out}(-\Omega_0) + \delta Y_{i1}^{\rm out}(\Omega_0)| \simeq {\rm e}^{r} > 1$. Figure 2(d) is the phase-squeezed state, in which the output signal field and the idle field are in phase, corresponding to the parametric amplification for the OPO. Thus, the coherent am-

plitude is larger than that in Figure 2(b) ($|\alpha_{s1}^{\rm out}| + |\alpha_{i1}^{\rm out}| = {\rm e}^{r}\alpha_{s1}^{\rm in} > \alpha_{s1}^{\rm in}$) and the noise amplitude distribution is opposite to that in Figure 2(c), i.e., the correlated noise amplitude $|\delta X_{s1}^{\rm out}(-\Omega_0) + \delta X_{i1}^{\rm out}(\Omega_0)| \simeq {\rm e}^{r} > 1$ when $\phi = \pm n\pi$, and $|\delta Y_{s1}^{\rm out}(-\Omega_0) + \delta Y_{i1}^{\rm out}(\Omega_0)| \simeq {\rm e}^{-r} < 1$ when $\phi = \pm n\pi + \pi/2$.

Figure 2(f)-(h) show the noise traces for the single-sideband injection at 5.0001 MHz, corresponding to case 2. Figure 2(f) shows the result for blocking the pump field of the OPO. It is a classical beat signal at $\Delta\Omega = 100$ Hz of the demodulation signal ($\Omega_0 = 5$ MHz) and the beat signal ($\Omega_0 + \Delta\Omega$) of the local field and the sideband fields, and is simultaneously modulated by a slow signal $\phi(t)$ on the phase. The coherent amplitude and the noise amplitude are similar to Figure 2(b). Figure 2(g) and (h) present the data when the pump is open. Obviously, these results are similar to the squeezed vacuum state because of the discrepancy between the modulation frequency and the demodulated frequency. In Figure 2(g), the phase θ of the pump and the input signal field is $\pi/2$, and hence the output signal field and the idle field of the OPO are out of phase. Thus, when $\phi(t) = \pm n\pi$, the coherent amplitude of the photocurrent subtraction is proportional to ${\rm e}^{-r}$, which is exactly the squeezing value of the OPO. If $\phi(t) = \pm n\pi + \pi/2$, the coherent amplitude of $i_{-2}(\Omega_0)$ is approximately proportional to ${\rm e}^{r}$, which corresponds to the parametric amplification for the OPO. Simultaneously, the noise amplitudes in the two figures illustrate the quantum correlation between the two output fields and have the same property as in case 1 discussed above. Thus, the coherent amplitude and the noise amplitude distribution in Figure 2(g)-(h) display the property of the squeezed vacuum state with more apparent effect. Similar to Figure 2(g)-(h), Figure 2(f) can be the analogy of the vacuum state.

Figure 3 shows the noise traces of the coherent state, the amplitude-squeezed state and the phase-squeezed state with double sidebands injection. Figure 3(b)-(d) represent the results for symmetric double sidebands injection when the frequency shift of AOM2 and AOM3 are 105 and 115 MHz respectively. The noise traces are similar to that shown in Figure 2(b)-(d) except for the double coherent amplitude. This case is equivalent to the traditional optical tomography scheme. Figure 3(f)-(h) show the corresponding results when the frequency shift of AOM2 and AOM3 are 105 and 115.0001 MHz respectively. The noise distribution and the coherent amplitude are just the sum of the noise traces in case 1 (Figure 2(b)-(d)) and case 2 (Figure 2(f)-(h)). These figures are the simulations of the coherent state, the amplitude-squeezed state and the phase-squeezed state and well present the properties of these states.

In our experiment, the classical gain is 1.8 when the single signal field slightly detuned from the fundamental frequency is fed in the OPO. Hence, the theoretical value of the squeezing parameter $r \approx 0.8$. However, the experimental value of r is about 0.4, which is smaller than the theoretical value because of the losses. In our experimental system, the intracavity loss is about 2%, the propagation loss is 25%, the interference visibility of the local field and the detected field is 95% and the quantum efficiency of the detector is about 0.9.

We experimentally studied the property of the quantum state by adopting the controllable sideband injection scheme and demonstrated that it is effective and useful in quantum state measurement. This scheme will be a powerful aid and can be used in quantum information processing, for example, to confirm the quantum state and the property and to build the forward feedback of quantum communication and quantum error correction.

This work was supported by the National Natural Science Foundation of China (NSFC) (Grant Nos. 11234008, 11361161002, 61571276, and 11654002), Natural Science Foundation of Shanxi Province (Grant No. 2015011007), and Shanxi Scholarship Council of China (Grant No. 2015-002).

1 R. E. Slusher, L. W. Hollberg, B. Yurke, J. C. Mertz, and J. F. Valley, Phys. Rev. Lett. **55**, 2409 (1985).
2 A. Furusawa, J. L. Sørensen, S. L. Braunstein, C. A. Fuchs, H. J. Kimble, and E. S. Polzik, Science **282**, 706 (1998).
3 H. Yan, and J. F. Chen, Sci. China-Phys. Mech. Astron. **58**, 074201 (2015).
4 X. L. Su, S. H. Hao, X. W. Deng, L. Y. Ma, X. J. Jia, C. D. Xie, and K. C. Peng, Nat. Commun. **4**, 2828 (2013).
5 X. Hu, H. Fan, D. L. Zhou, and W. M. Liu, Phys. Rev. A **85**, 032102 (2012).
6 Z. G. Li, S. M. Fei, Z. D. Wang, and W. M. Liu, Phys. Rev. A **79**, 024303 (2009).
7 D. Blair, L. Ju, C. N. Zhao, L. Q. Wen, H. X. Miao, R. G. Cai, J. R. Gao, X. C. Lin, D. Liu, L. A. Wu, Z. H. Zhu, G. Hammond, H. J. Paik, V. Fafone, A. Rocchi, C. Blair, Y. Q. Ma, J. Y. Qin, and M. Page, Sci. China-Phys. Mech. Astron. **58**, 120405 (2015).
8 R. Schnabel, N. Mavalvala, D. E. McClelland, and P. K. Lam, Nat. Commun. **1**, 121 (2010).
9 V. Giovannetti, S. Lloyd, and L. Maccone, Nat. Photon. **5**, 222 (2011).
10 J. Bertrand, and P. Bertrand, Found Phys. **17**, 397 (1987).
11 G. Breitenbach, S. Schiller, and J. Mlynek, Nature **387**, 471 (1997).
12 G. M. D'Ariano, M. Vasilyev, and P. Kumar, Phys. Rev. A **58**, 636 (1998).
13 J. Zhang, T. Zhang, K. Zhang, C. Xie, and K. Peng, J. Opt. Soc. Am. B **17**, 1920 (2000).
14 H. Fan, D. He, and S. Feng, J. Opt. Soc. Am. B **32**, 2172 (2015).
15 W. Li, X. D. Yu, Z. M. Meng, Y. B. Jin, and J. Zhang, Sci. China-Phys. Mech. Astron. **58**, 104201 (2015).
16 T. A. Wheatley, D. W. Berry, H. Yonezawa, D. Nakane, H. Arao, D. T. Pope, T. C. Ralph, H. M. Wiseman, A. Furusawa, and E. H. Huntington, Phys. Rev. Lett. **104**, 093601 (2010).
17 W. Li, X. D. Yu, and J. Zhang, Opt. Lett. **40**, 5299 (2015).
18 L. A. Wu, H. J. Kimble, J. L. Hall, and H. Wu, Phys. Rev. Lett. **57**, 2520 (1986).
19 K. Di, X. D. Yu, and J. Zhang, Acta Sin. Quantum Opt. **16**, 241 (2010).
20 X. D. Yu, W. Li, Y. B. Jin, and J. Zhang, Sci. China-Phys. Mech. Astron. **57**, 875 (2014).
21 S. Chelkowski, H. Vahlbruch, K. Danzmann, and R. Schnabel, Phys. Rev. A **75**, 043814 (2007).